

Chapter 3

Effect of constitutive expression of *Vitreoscilla*
hemoglobin on biofilm formation and sporulation
in
Bacillus subtilis DK1042

3.1 Introduction

Bacillus subtilis is the model system demonstrating development and differentiation in simple prokaryotes. Cellular differentiation comprises different cell cycle events such as motile growth, competence, biofilm formation and sporulation (Lopez et al., 2009). Onset of each event is governed by gradual increase in the level of master regulator Spo0A~P. At low level of Spo0A~P, cells remain motile, intermediate level of Spo0A~P induces matrix production genes and at high levels cells undergo sporulation (Vlamakis et al., 2013). Biofilm formation is a protective mechanism to withstand environmental challenges (Costerton et al., 1995; Ciofu and Tolker-Nielsen, 2019). Low oxygen concentration impairs aerobic respiration in *B. subtilis* that leads to matrix production and consequent colony wrinkling by *B. subtilis* (Kolodkin-Gal et al., 2013). Similar colony wrinkling is triggered by a combination of glycerol and manganese (GM) in lysogeny broth (LB) medium (Shemesh and Chai, 2013). Colony wrinkling is an adaptation that increases the surface to volume ratio facilitating greater access to oxygen in response to decreased oxygen concentration. *Vitreoscilla* hemoglobin (VHb) improves aerobic growth and bioproduct synthesis by supplying oxygen to the respiratory chain (Stark et al., 2015). Heterologous expression of VHb improved cell growth and total protein secretion, insecticidal crystal protein yields, γ -PGA production and biodegradation of phenol and p-nitrophenol in *B. subtilis*, *B. thuringiensis*, *B. amyloliquefaciens* and *B. cereus*, respectively (Kallio and Bailey, 1996; Feng et al., 2007; Zhang et al., 2013; Velez-Lee et al., 2015).

In *B. subtilis*, biofilm formation is a very well-orchestrated process involving expression of multicistronic *epsA-O* and the *tapA-sipW-tasA* operons coding for exopolysaccharide (EPS) and amyloid fiber (TasA) components, respectively, of the biofilm matrix (Cairns et al., 2014). Expression of these operons is under negative control by SinR and AbrB. Low to intermediate levels of Spo0A~P represses expression of *abrB* and turns on the synthesis of two anti-repressor proteins SinI and AbbA which derepress the genes under the control of SinR and AbrB, respectively (Banse et al., 2008). Spo0A is activated by phosphorylation via a multicomponent phosphorelay involving five sensory histidine kinases (KinA–E), Spo0F and Spo0B in response to various environmental signals (Jiang et al., 2000). In addition to EPS and TasA, bacterial hydrophobin encoded by *bslA* gene is yet another extracellular component of *B. subtilis* biofilm that acts

synergistically with EPS and TasA to form robust biofilm (Cairns et al., 2014). BslA is responsible for the apparent complexity and extreme hydrophobicity displayed by the mature biofilm. Production of BslA is directly repressed by AbrB (Verhamme et al., 2009) and indirectly activated by Rok (Kovacs and Kuipers, 2011) as well as intermediate level of DegU~P. DegU has different regulatory activities in its phosphorylated (DegU~P) and non-phosphorylated (DegU) forms. DegU and low level of DegU~P activates genetic competence and motility, respectively (Hamoen et al., 2000; Kobayashi 2007). Intermediate level of DegU~P shuts off motility genes and activates biofilm formation while very high amount of DegU~P inhibits biofilm formation and leads the cells towards terminal developmental stage of sporulation by affecting the level of Spo0A~P (Marlow et al., 2014). Thus, DegU and Spo0A both contribute to the cell differentiation process manifested by *B. subtilis* in a similar fashion by employing their ability to bind low and high affinity target promoters in response to wide array of input signals (Murray et al., 2009; Verhamme et al., 2009).

3.2 Rationale

Oxygen scarcity is known to induce complex biofilm formation in some bacteria including *B. subtilis* (Dietrich et al. 2008, Dietrich et al. 2013; Kolodkin-Gal et al., 2013). However, the effect of one of the most studied oxygen carrier – VHb on multicellularity is not investigated in detail in *Bacillus* spp.. In order to study the effect of VHb independent of any regulatory mechanisms, it was expressed constitutively under the control of most widely used *P43* promoter (Wang and Dio, 1984) in *B. subtilis* DK1042. Single copy integration of target genes under strong promoter is insufficient to achieve the higher yield of the protein. Li et al. (2012) described a potential method to increase the expression of target genes by using multiple promoter repeats upstream of the desired gene cassettes. Similarly, multiple repeats of *P43* promoter were used upstream of the *vgb-gfp* operon to enhance the expression of these genes. Here, we report that genomic integration of *vgb* in *B. subtilis* DK1042 mitigates architectural complexity of biofilm formation and associated sporulation under different conditions.

3.3 Work plan

3.3.1 Bacterial Strains used in this study

Table 3.1: Bacterial strains used and constructed in this study

Bacterial Strains	Genotype	Reference
<i>E. coli</i> DH10B	<i>FendA1 recA1 galE15 galK16 nupGrpsL ΔlacX74 Φ80lacZΔM15 araD139 Δ (ara, leu) 7697 mcrA Δ(mrr-hsdRMS-mcrBC)</i> ^{λ-}	Invitrogen
DH10B (pNRM1)	<i>E. coli</i> DH10B with plasmid pNRM1; Amp ^r	This study
DH10B (pNRM2)	<i>E. coli</i> DH10B with plasmid pNRM2; Amp ^r	This study
DH10B (pNRM11)	<i>E. coli</i> DH10B with plasmid pNRM11; Amp ^r ; Km ^r ; Neo ^r	This study
DH10B (pNRM157)	<i>E. coli</i> DH10B with plasmid pNRM157; Amp ^r ; Km ^r ; Neo ^r	This study
DH10B (pNRM1113)	<i>E. coli</i> DH10B with plasmid pNRM1113; Amp ^r ; Km ^r ; Neo ^r	This study
DH10B (pNRM1114)	<i>E. coli</i> DH10B with plasmid pNRM1114; Amp ^r ; Km ^r ; Neo ^r	This study
DH10B (pNRM13)	<i>E. coli</i> DH10B with plasmid pNRM13; Amp ^r ; Km ^r ; Neo ^r	This study
DH10B (pNRM14)	<i>E. coli</i> DH10B with plasmid pNRM14; Amp ^r ; Km ^r ; Neo ^r	This study
<i>B. subtilis</i> DK1042	NCIB 3610 <i>ComI</i> ^{Q12L}	BGSC, Konkol et al., 2013
NRM1113	<i>B. subtilis</i> DK1042 <i>amyE::P43-lox71-Kan-lox66-P43-vgb-gfp</i>	This study
NRM1114	<i>B. subtilis</i> DK1042 <i>amyE::P43-lox71-Kan-lox66-(P43)₄-vgb-gfp</i>	This study

3.3.2 Cloning of promoterless *gfp* in pUC19

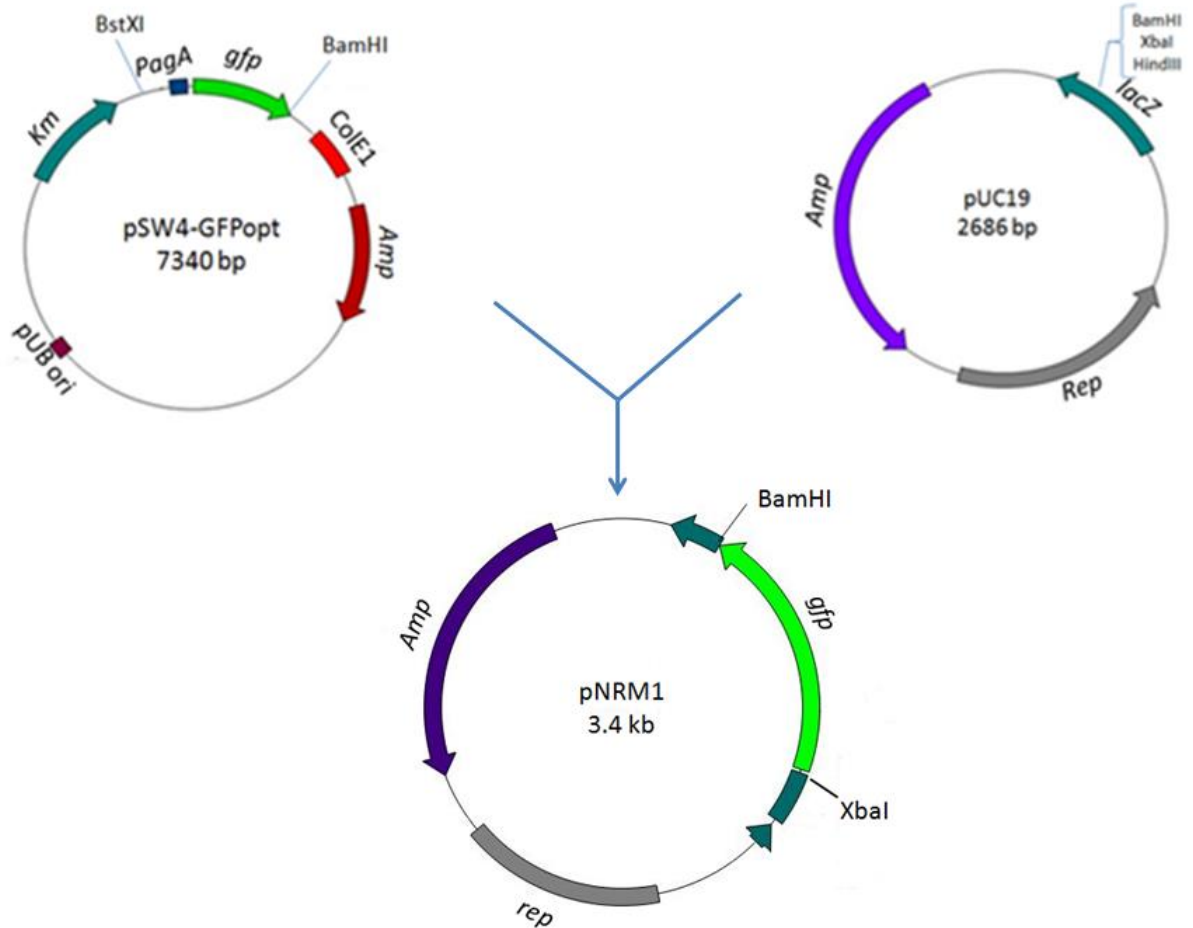


Fig. 3.1: Schematic representation for cloning of promoterless *gfp* in pUC19

gfp gene was PCR amplified using *gfpF/gfpR* from pSW4 using gene specific primers having XbaI/BamHI restriction sites, followed by ligation into pUC19 to give rise to pNRM1 plasmid. Primer sequences used for cloning of *gfp* gene are as follow; restriction sites are italicised and ribosome binding site (RBS) are underlined.

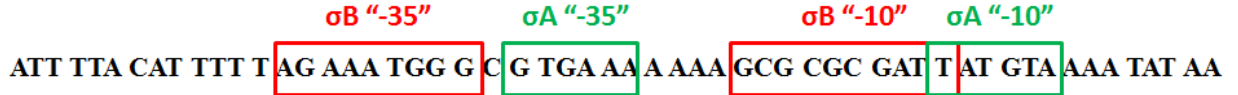
gfpF: 5' - GCT CTA *GAGCAT* ATT AAG AGG AGG AGA ATA CAA ATG TCA AAA
GGA GAA GAA TTA TTT ACA GGG GTA GT - 3'

gfpR: 5' - CGG *GAT CCG* CTG CAC TGC AGG TCA CGA GCT CGT TAC TTA TAT
AAT TCA TCC ATT CCG TGT GTA ATT CCT GC - 3'

3.3.3 Construction of plasmid pNRM2 containing P43-*vgb*-*gfp* operon

3.3.3.1 Sequence and regulatory features of P43 promoter

P43 is a 56 bp long, strong constitutive promoter (Zhang et al., 2005). It was cloned upstream of *vgb* gene by overlap extension PCR.



3.3.3.2 Cloning of P43-*vgb* upstream of *gfp* in pNRM1

Two different forward primers and a reverse primer were designed to clone *vgb* and to incorporate *P43* promoter. Primer sequences are as follow; restriction sites are italicised and RBS are underlined. *P43* promoter sequence is highlighted in red colour and overlapping region between both the forward primers is highlighted in bold.

*vgb*F1: 5'- CC AAG *CTTATT TTA CAT TTT TAG AAA TGG GCG TGA AAA AAA GCG CGC GAT TAT GTA AAA TAT AAA TAA AGT GAT ATA TTA AGA GG AGG AG* -3'

*vgb*F2: 5' - **GC GAT TAT GTA AAA TAT AA**ATA AAG TGA TAT ATT AAG AGG AGG AGGAC CCT CAT GTT AGA CCA GCA AAC – 3'

*vgb*R: 5'- TGC *TCT* AGA TTA TTC AAC CGC TTG AGC GTA CAA ATC TG -3'

vgb was amplified using *vgb*F2 and *vgb*R from pUC8:15 plasmid containing *vgb* gene. *vgb*F2R amplicon was purified using PCR clean up kit (Nucleopore Quick PCR Purification Kit, Gentix Biotech Asia Pvt. Ltd.) and this purified amplicon was used as template to incorporate complete sequence of *P43* promoter using *vgb*F1 and *vgb*R primers. The amplicon obtained after second PCR was designated as *vgb*F1R. Thus, *vgb*F1R consisted of forward restriction site HindIII - *P43* promoter – RBS – *vgb* and reverse restriction site XbaI. *vgb*F1R amplicon was digested with HindIII and XbaI and was ligated into pNRM1 to give rise to pNRM2. Thus, pNRM2 contains bicistronic operon containing *vgb* and *gfp* gene under the control of constitutive *P43* promoter.

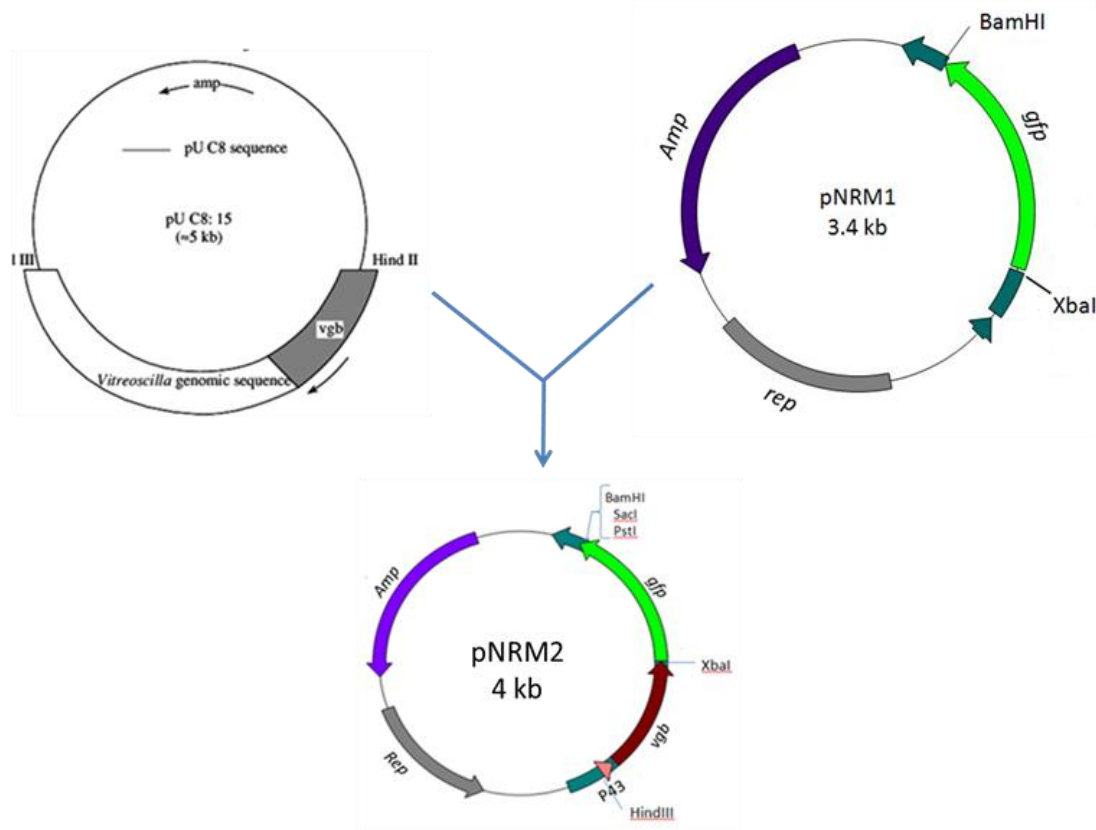


Fig. 3.2: Schematic representation for cloning of P43-*vgb* operon upstream of *gfp* in pNRM1

3.3.4 Construction of different integration vectors

3.3.4.1 Replacement of kanamycin resistance gene with *Km^r-lox* cassette for provision of marker removal

pDK is an *amyE* locus based integration vector (Yuan and Wong, 1995). In order to obtain marker-less integrants of *B. subtilis* DK1042, kanamycin resistance gene (*Km^r*) of pDK was replaced with *P43-lox71-Km^r-lox66* cassette. *Cre/lox* is very efficient genetic tool to introduce various genetic modifications such as insertion, deletion and inversion (Dong and Zhang, 2014). Mutant *lox* sites *lox71* and *lox66* are used to decrease the genetic instability because a double mutant *lox72* site, which has weaker binding affinity for Cre, is obtained following recombination of *lox71* and *lox66*, allowing for repeated mutations in a single genetic background (Albert et al., 1995; Suzuki et al., 2005; Lambert et al., 2006). After integration of desired gene

cassettes into the chromosome, the antibiotic marker can be removed by transient expression of Cre using temperature sensitive helper plasmid (Yan et al., 2008).

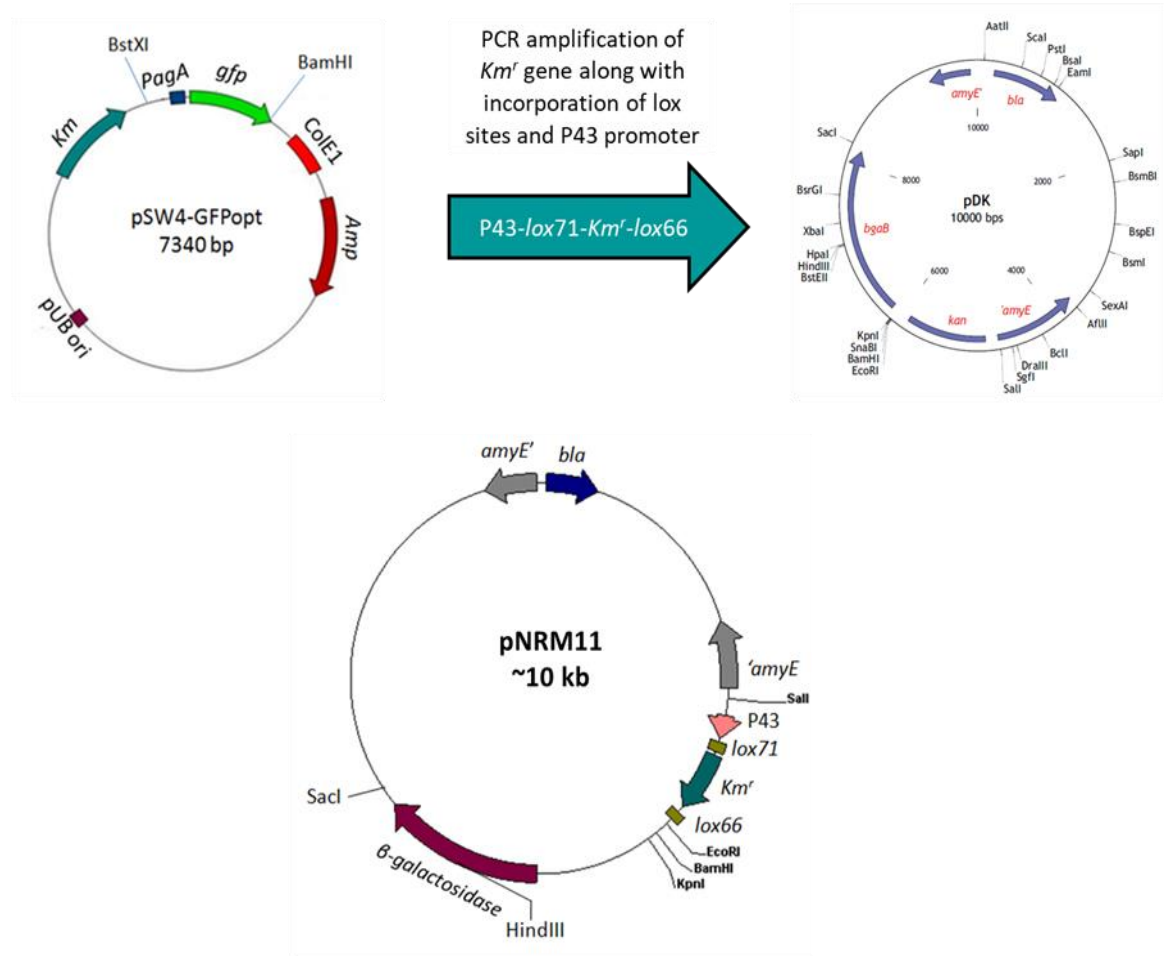


Fig. 3.3: Schematic representation of construction of pNRM11 integration vector

Directly repeated mutant *lox* sites *lox71* and *lox66* flanking *Km^r* incorporated using overlapping extension PCR. *P43-lox71-Km^r-lox66* cassette was generated by amplifying the *Km^r* gene with three different forward primers and a reverse primer. The sequences of gene specific primers are as follow; restriction sites are italicized, RBS is underlined, *P43* promoter id highlighted with red font, *lox71* site is highlighted in yellow background and *lox66* site is highlighted in gray background, overlapping regions between two primers are highlighted in bold characters.

KAN1F –5’ –**CAT ACA TTA TAC GAA GTT ATA TAT TAA GAG GAG GAG**
AAT ACA AAT GAG AAT AGT GAA TGG ACC AAT AAT AAT GAC TAG AGA
AGA AA – 3’

KAN2F – 5’ - **AAA GCG CGC GAT TAT GTA AAA TAT AAT ACC GTT CGT**
ATA GCA TAC ATT ATA CGA AGT TAT ATA TTA AGA GG AGG AGA ATA
CAA ATG AGA – 3’

KAN3F – 5’ – CGC *GTC GAC* **ATT TTA CAT TTT TAG AAA TGG GCG TGA**
AAA AAA GCG CGC GAT TAT GTA AAA TAT AAT ACC GTT C -3’

KANR – 5’ – CCG *GAA TTC* TAC CGT TCG TAT AAT GTA TGC TAT ACG AAG
TTA TTC AAA ATG GTA TGC GTT TTG ACA CAT CCA CTA TAT ATC- 3’

3.3.4.2 Cloning of tandem repeats of P43 promoters in pNRM11

Plasmid transformants can express proteins in higher amount and these proteins can be utilized to achieve the desired functions with greater efficiency because of higher copy number of genes attributed by high copy number of plasmids. However, there are some limitations associated with the plasmid based expression of gene, such as genetic instability, structural instability, metabolic burden (Lin-Chao and Bremer, 1986; Friehs, 2004; Rozkov et al., 2004; Buch et al., 2010). Genomic integration of genes provides better stability and it obviates the use of antibiotics. Current study was aimed at improving the biofertilizer potential of resulting *B. subtilis* DK1042 in the natural environment, therefore stable integration of desired gene cassettes was the method of choice. Though chromosomal integration provides a better solution to the stability problem, single copy integration reduces the expression of genes as compared to that of plasmid based expression. Tyo et al., (2009) devised the strategy termed as chemically inducible chromosomal evolution method (CICHE) wherein the strain carrying the desired genes along with the antibiotics integrated into the chromosome was subjected to adaptive evolution by gradually increasing antibiotic concentration in the medium to obtain high copies in the locus. This was the plasmid-free approach that enhanced efficiency of metabolic engineering, but increase in the copies of the target gene and an antibiotic resistance gene also resulted in the significant increase in the

redundant DNA. These DNA sequences may pose metabolic burden for the host (Kolisnychenko et al., 2002). Li et al., (2012) developed a strategy to increase the production of polyhydroxybutyrate (PHB) in *E. coli* without increasing the amount of superfluous DNA. It was achieved through improved transcription strength by constructing the promoter clusters consisting of multiple core-tac promoters. Integration of the *phbCAB* genes comprising 4.3 kb length under the control of five core tac promoter clusters (CPTacs) resulted in an engineered *E. coli* that can accumulate 23.7% PHB of the cell dry weight in batch cultivation. Tandem repeats of *P43* promoter were generated by gene synthesis and were cloned in pNRM11 between *EcoRI* and *BamHI* sites to give rise to pNRM157.

Sequence of tandem repeat consisting of 3 P43 promoters:

GAATTCATTTTACATTTTTAGAAATGGGCGTGAAAAAAGCGCGCGATTAT
GTAAAATATAAATTTTACATTTTTAGAAATGGGCGTGAAAAAAGCGCGC
GATTATGTAAAATATAAATTTTACATTTTTAGAAATGGGCGTGAAAAA
GCGCGCGATTATGTAAAATATAAGGATCC

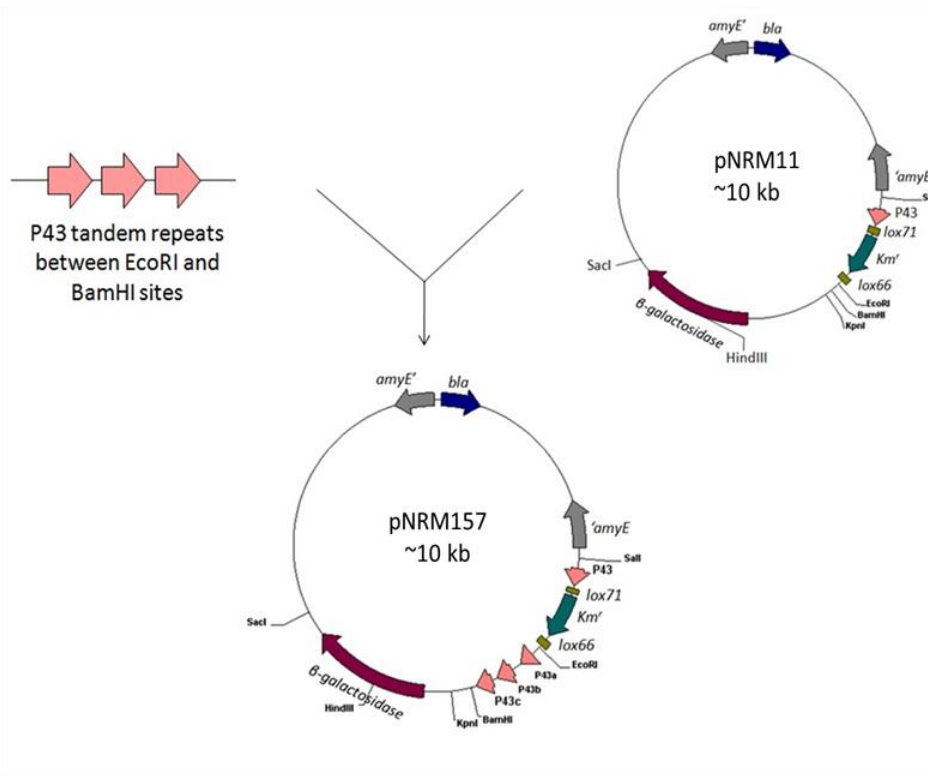


Fig.3.4: Schematic representation for construction of integration vector with P43 repeats

3.3.4.3 Cloning *vgb-gfp* operon in the integration vector

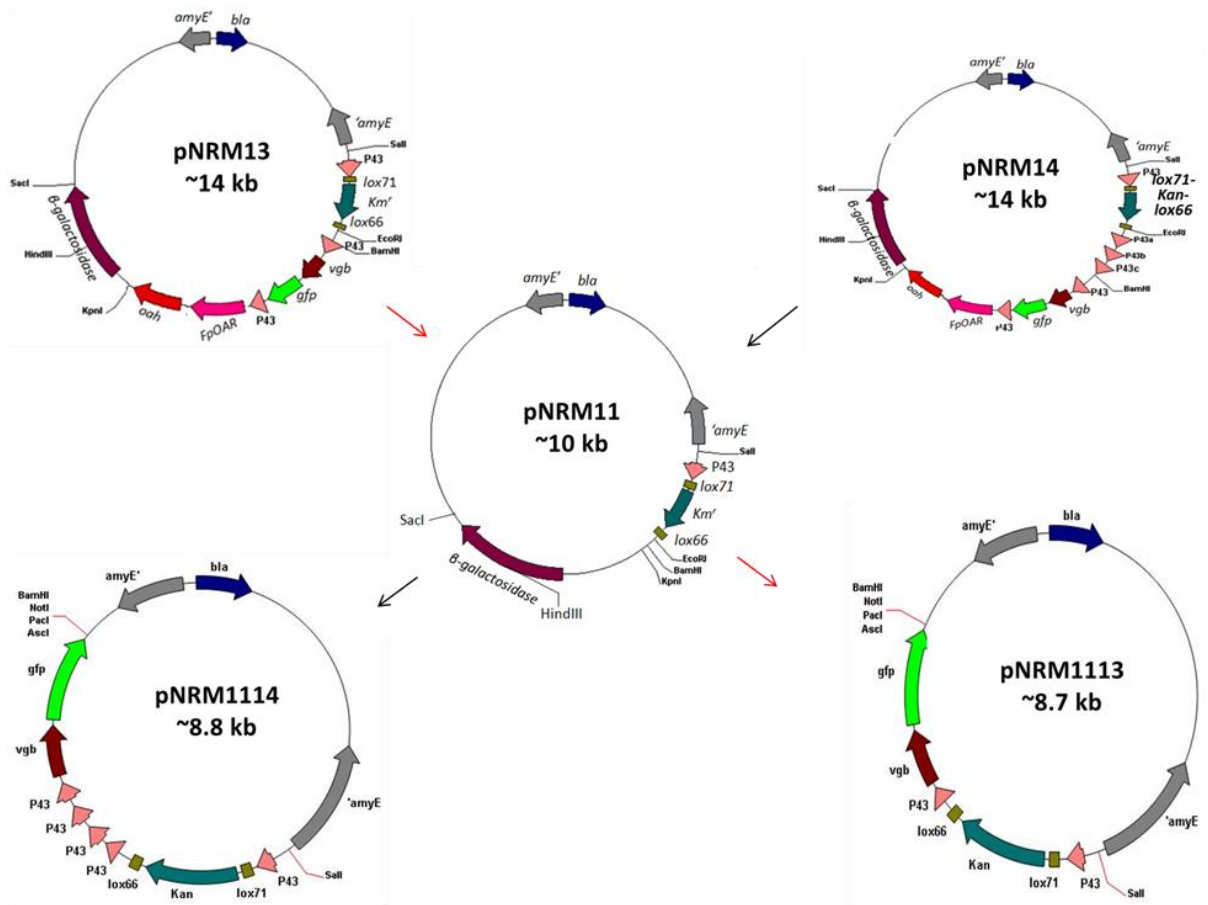


Fig. 3.5: Schematic representation for construction of integration vector pNRM1113 and pNRM1114

Vector pNRM11 was digested with SalI and SacI followed by treatment with Klenow to generate the blunt ends. *P43-lox71-kan-lox66 - P43-vgb-gfp* and *P43-lox71-kan-lox66 - (P43)₃-(P43)-vgb-gfp* fragments were PCR amplified using *vgbF1KpnI* and *gfpR16* primers from pNRM13 and pNRM14 respectively and were ligated to above mentioned blunt end digested pNRM11 to give rise to pNRM1113 and pNRM1114 respectively.

3.3.5 Transformation of *E. coli* and *B. subtilis* DK1042 with respective vectors

3.3.5.1 Development of *E. coli* transformants harboring plasmid pNRM1, pNRM2, pNRM11, pNRM157, pNRM1113 and pNRM1114

As mentioned in section 2.3.7.1, *E. coli* DH10B was transformed using MgCl₂-CaCl₂ method (Sambrook and Russell 2001). All the plasmid transformants were screened for ampicillin resistance (Amp^r).

3.3.5.2 Development of *B. subtilis* DK1042 integrants harboring plasmid pNRM1113 and pNRM1114

As mentioned in section 2.3.7.2, *B. subtilis* DK1042 was transformed with the integration vectors pNRM1113 and pNRM1114 using natural competence method and the integrants thus obtained were designated as NRM1113 and NRM1114 respectively. The *Km^r* gene also confers resistance to neomycin antibiotic in *B. subtilis* DK1042 therefore; the integrants were screened for neomycin resistance and neomycin resistant colonies of *B. subtilis* DK1042 were then reconfirmed for integration at *amyE* and not any other place in the genome using starch agar plate.

3.3.6 Evaluation of transcription efficiency of P43 tandem repeats using GFP fluorescence assay

Effect of promoter repeats on target gene expression was monitored by GFP fluorescence of integrants in a time dependent manner in Luria Bertani and M9 broth (Kleign et al., 2010) at 200 rpm at 37°C. One ml of bacterial culture was taken out every 2 h and harvested by centrifugation at 10000 rpm for three minutes followed by resuspension in 0.85% Saline. O.D.₆₀₀ and fluorescence (excitation at 470 nm and emission at 515±20 nm) were measured.

3.3.7 Effect of *Vitreoscilla* hemoglobin (VHb) on biofilm formation and sporulation in *B. subtilis* DK1042

As mentioned in section 2.2.4 and 2.6, biofilm formation by *B. subtilis* DK1042 (henceforth WT) and VHb harboring integrants NRM1113 and NRM1114 was studied in following four different media: Lysogeny Broth (LB), LB medium containing 6 %

NaCl, biofilm-promoting LBGM medium and Mmsg medium. Biofilm-associated sporulation was studied in colony biofilms of WT and NRM1113 grown on LB and LBGM agar medium as shown in the section 2.6.

3.4 Results and Discussion

3.4.1 Construction of various plasmids and integration vector

Cloning of different genes in different vectors was confirmed by restriction digestion pattern analysis post cloning.

3.4.1.1 Construction of pNRM1

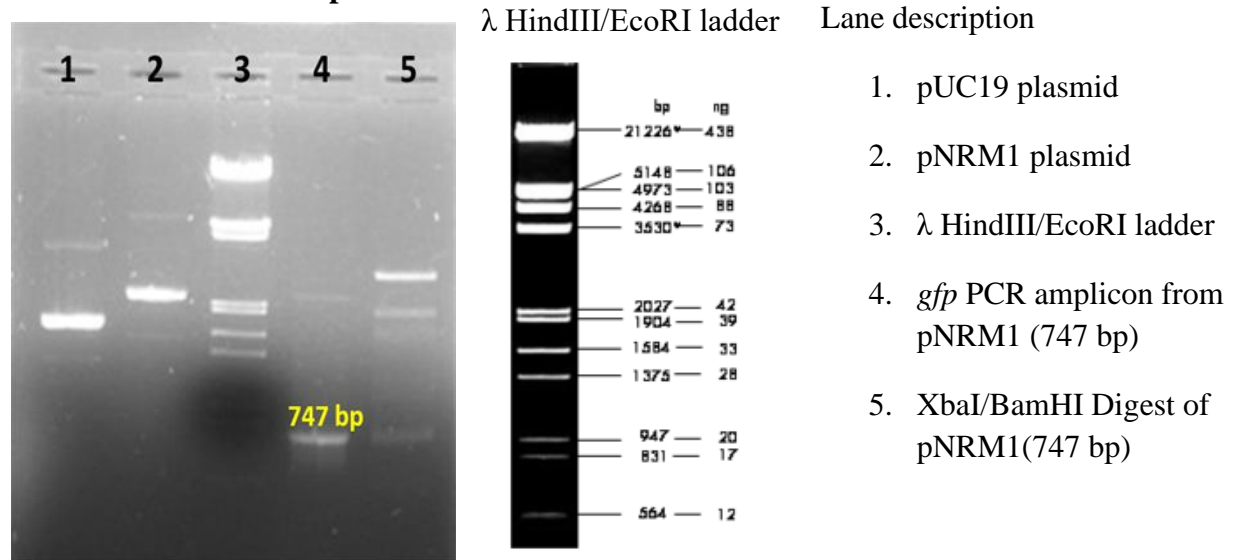


Fig. 3.6: PCR amplification and restriction digestion confirmation of pNRM1

3.4.1.2 Construction of pNRM2

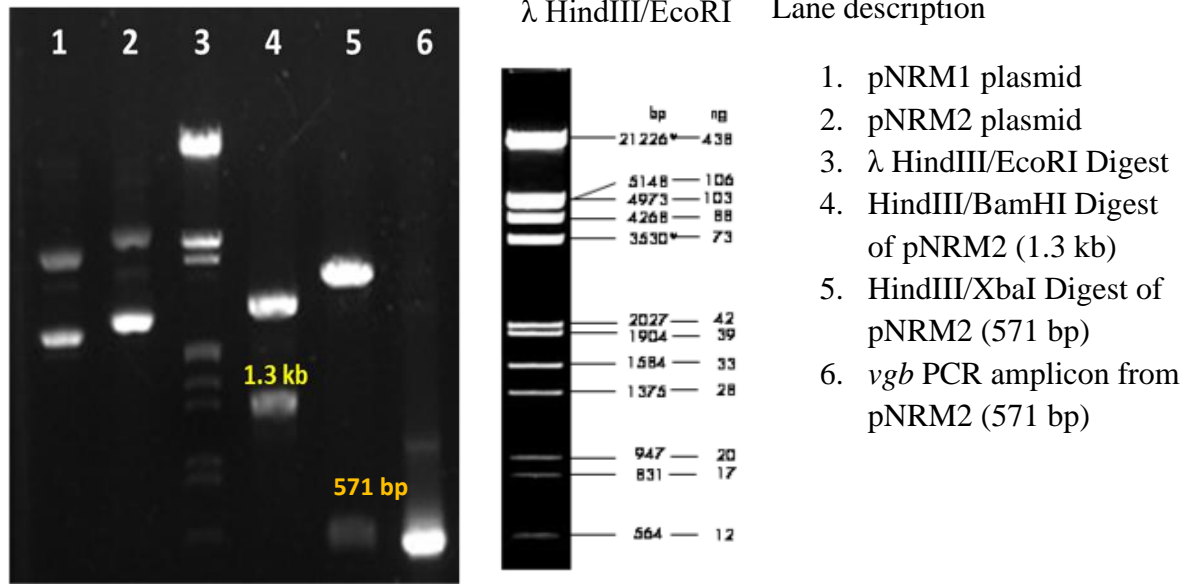


Fig. 3.7: PCR amplification and restriction digestion confirmation of pNRM2

3.4.1.3 Construction of pNRM11

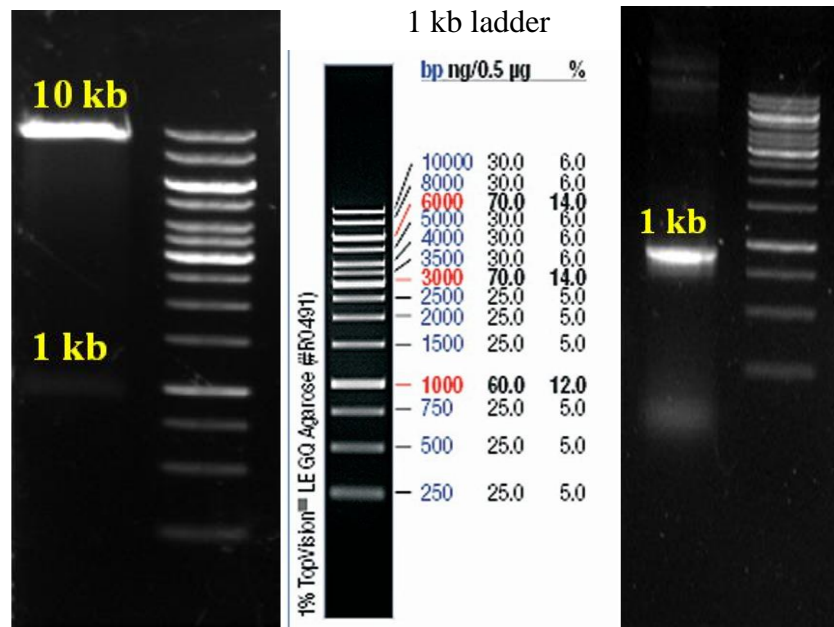


Fig. 3.8: (A) - Restriction digestion SalI/EcoRI of pNRM11, (B) - PCR amplification of P43-*lox71*-*Km'*-*lox66*

3.4.1.4 Construction of pNRM157

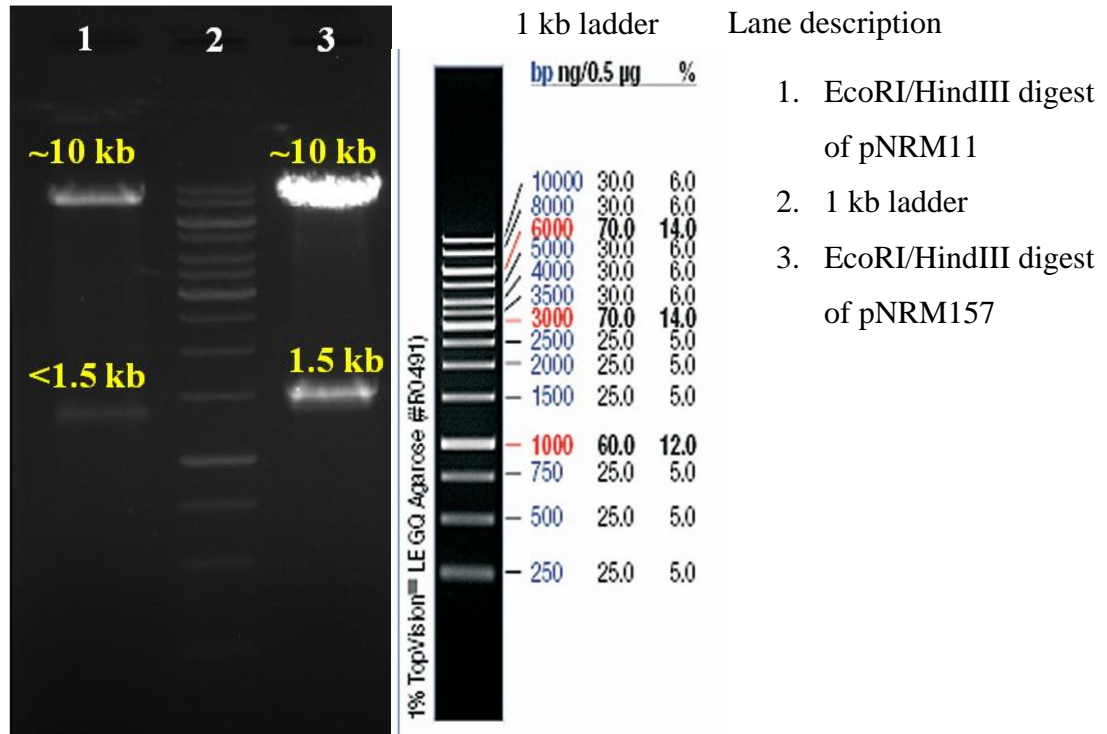


Fig. 3.9: Restriction digestion of pNMR157

The length of *P43* tandem repeats (*P43*)₃ is 180 bp and it is difficult to demonstrate the release of 180 bp from ~10 kb vector on agarose gel. So, cloning of *P43* tandem repeats downstream of *Km^r-lox* cassette was confirmed by comparing the restriction digestion pattern of pNRM11 and pNRM157 with the same restriction enzymes EcoRI and HindIII. Digestion of pNRM157 with EcoRI and HindIII restriction enzymes should result in the release of a fragment containing *P43-lox71-Km^r-lox66-(P43)₃*, which is 180 bp longer than that of the fragment *P43-lox71-Km^r-lox66*, released from the pNRM11 due to successful incorporation of *P43* repeats downstream of *Km^r-lox* cassette. As shown in **Fig. 3.9**, it was found that the size of the fragment released from pNRM157 was higher than that of released from pNRM11.

3.4.1.5 Construction of pNRM1113 and pNRM1114

P43-lox71-kan-lox66 - P43-vgb-gfp and *P43-lox71-kan-lox66 - (P43)₃-(P43)-vgb-gfp* fragments were cloned in pNRM11 via blunt end ligation to construct the integration vectors pNRM1113 and pNRM1114 respectively. Both these clones were

confirmed by colony PCR from the *E. coli* transformants and by comparing the length of the PCR amplicons obtained from pNRM1113 and pNRM1114 using KAN3F and *gfpR16* primers. As shown in **Fig. 3.10**, it was found that the size of the KAN3F-*gfpR16* amplicon obtained from pNRM1114 was higher than that of the KAN3F-*gfpR16* amplicon obtained from pNRM1113.

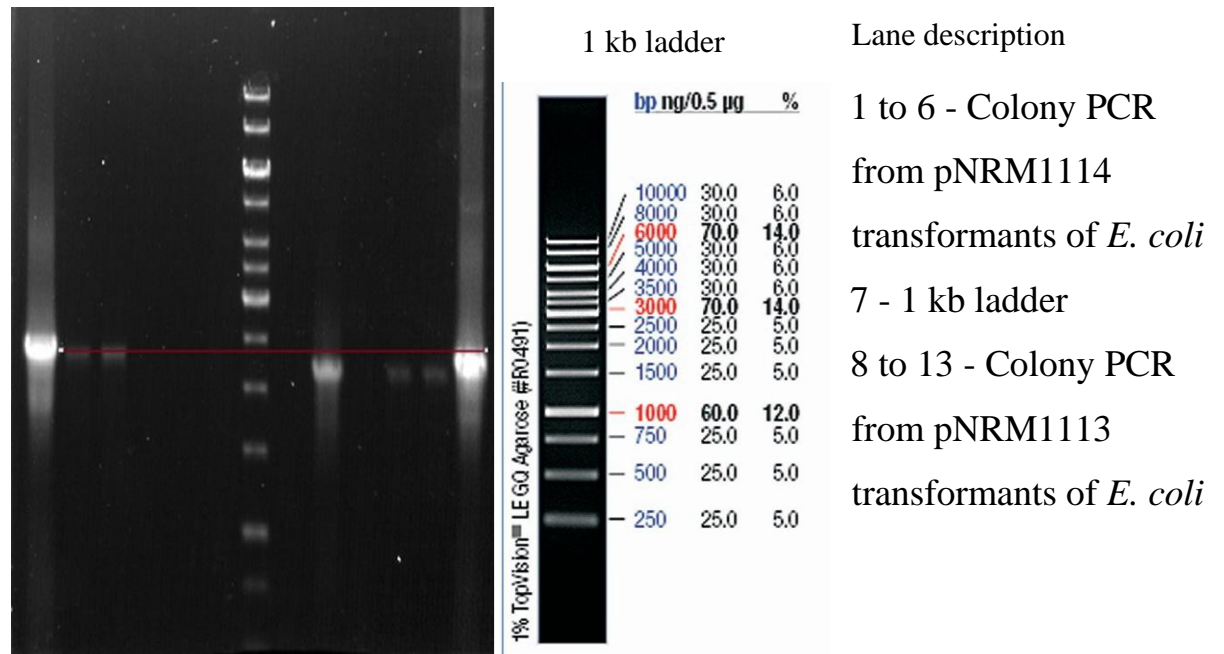


Fig. 3.10: Confirmation of incorporation of *vgb-gfp* operon under different P43 promoter setup

3.4.2 Selection of integrants DK1042 NRM1113 and NRM1114 using starch agar assay

As mentioned in section 2.3.7.2, double crossover homologous recombination events were confirmed by screening kanamycin resistant DK1042 colonies on starch agar plate for the absence of amylase activity (**Fig. 3.11**). Due to successful integration at *amyE* locus through double crossover homologous recombination, *amyE* locus in the genome of DK1042 is disrupted and absence of starch hydrolysis zone surrounding the integrant colonies facilitates the selection of correct integrants.

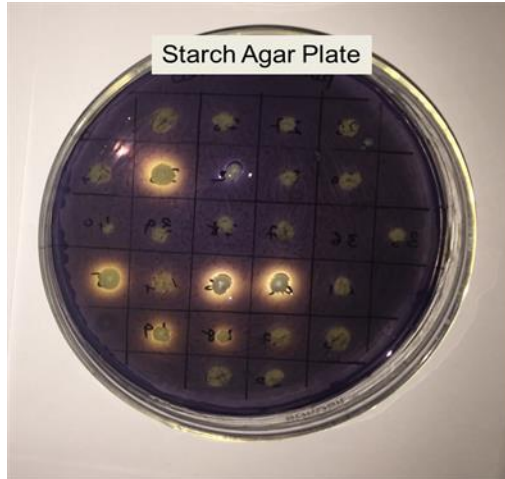


Fig. 3.11: Screening of kanamycin resistant colonies on starch agar plate.

3.4.3 Determining the strength of P43 promoter in NRM1113 and NRM1114

Effect of multiple *P43* promoters was determined by time dependent analysis of GFP fluorescence. Time dependent analysis of GFP Fluorescence/O.D.₆₀₀ ratio revealed that NRM1114 having five copies of *P43* promoter upstream of *vgb-gfp* operon showed two fold higher intensity than NRM1113 having two copies of *P43* promoter in both Luria Bertani and M9 minimal medium (**Fig. 3.12, A and B**)

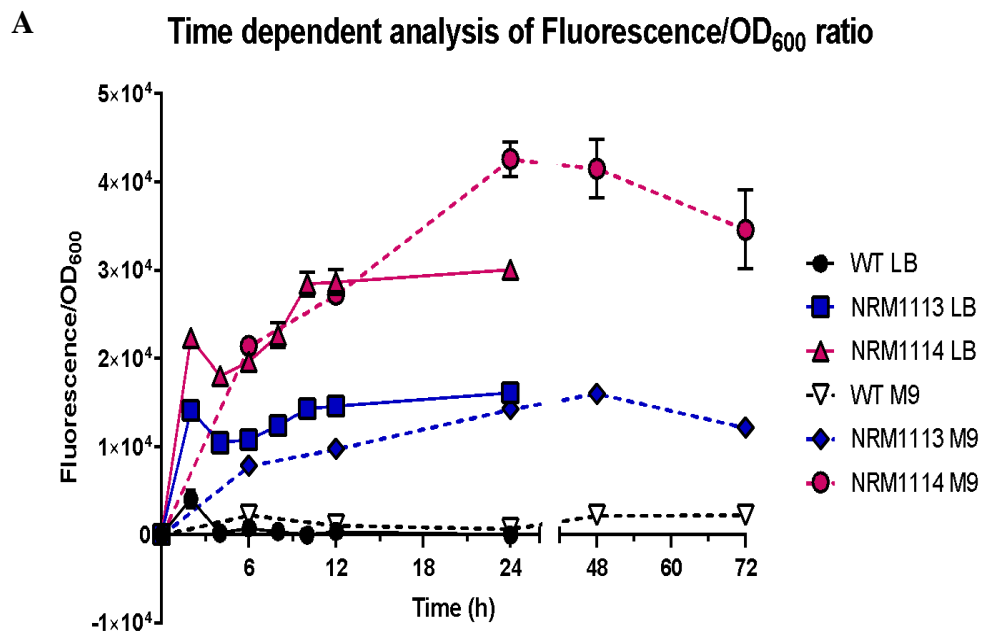


Fig. 3.12: (A) Time dependent analysis of GFP fluorescence

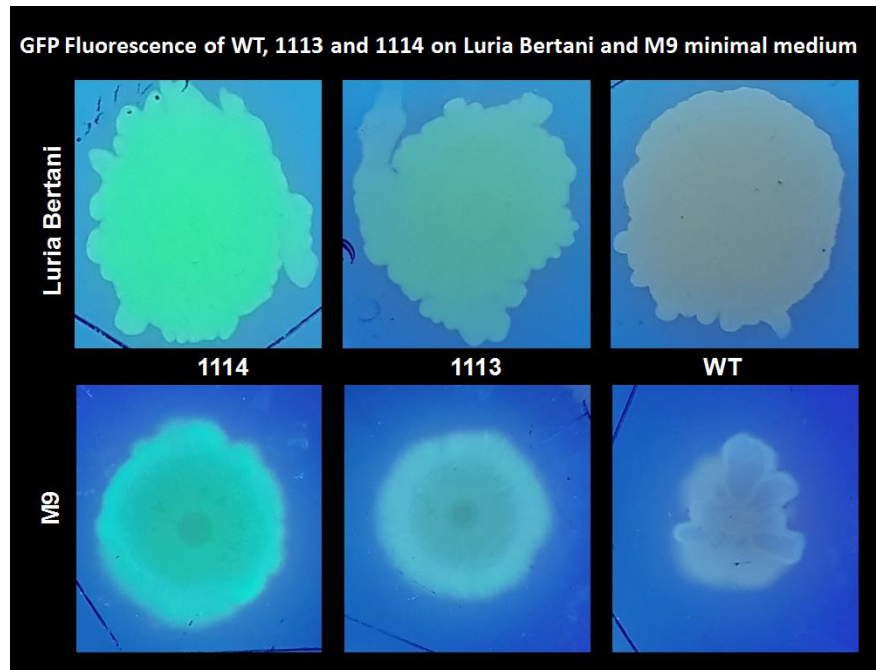
B

Fig. 3.12: (B) GFP Fluorescence on Luria Bertani and M9 minimal medium

3.4.4 Heterologous expression of VHb in *B. subtilis* DK1042 and its effect on biofilm formation, sporulation and brown pigment production

3.4.4.1 Alteration in biofilm formation and genetic basis thereof

Incorporation of VHb reduced complexity and increased the diameter of colony biofilm in NRM1113 as compared to WT on both LB and LBGM (**Fig. 3.13, A and Fig. 3.14, Panels 1 to 4**). However there was no significant difference in NRM1114 as compared to WT (**Fig. 3.14, Panel 1 and 2**) therefore, rest all the studies were conducted to compare NRM1113 and WT. Colony diameter of NRM1113 increased 2.83 and 1.95 fold with respect to WT on LB and LBGM respectively ($n = 3, P < 0.05$). Strikingly, surface spreading by NRM1113 was also observed on LB containing 4% NaCl (**Fig. 3.14, Panel 5**). In order to determine the reason for this surface spreading, WT and NRM1113 were assayed for growth in LB, LBGM and 6% NaCl LB broth. Growth curve experiments showed that both WT and NRM1113 followed similar growth trajectories but specific growth rate (μ) of NRM1113 was slightly higher than that of WT under all the experimental conditions which may contribute to the increased fitness of the integrant (**Fig. 3.15, Table 3.2**). Doubling time of NRM1113 was 9 min

shorter than that of WT under osmotic stress. Biofilm phenotype was also monitored on Mmsg medium where WT produced more wrinkled colonies as compared to NRM1113 after 24 h incubation. Morphological differences between these two were reduced with further incubation. Similar trend appeared in pellicles formed in Mmsg broth (Fig. 3. 16). Morphological difference was less significant between the colony biofilms of WT and NRM1113 grown on Mmsg medium in comparison to colonies grown on LB and LBGM possibly because Mmsg is a minimal medium containing glycerol and glutamate as the carbon source and glycerol is an energy poor carbon source in comparison to complex LB and LBGM media (Martinez-Gomez et al., 2012; Chubukov et al., 2013; Wang et al., 2015).

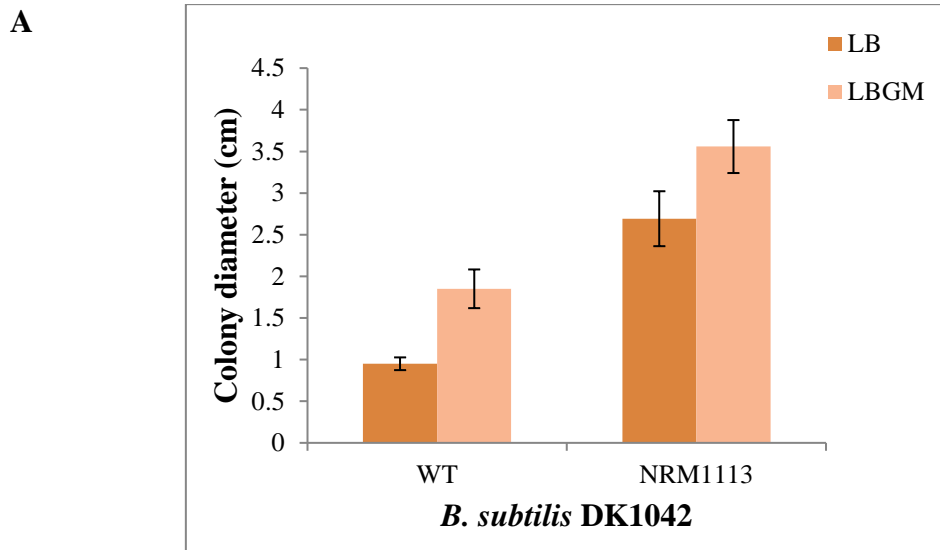


Fig. 3.13: Characterization of biofilm formation in *B. subtilis* DK1042 harbouring Vhb (A) Colony expansion of WT and NRM1113 on LB and LBGM agar (1.5%) medium at 72 h, (n=3, $p \leq 0.05$, error bars represent standard error of mean).

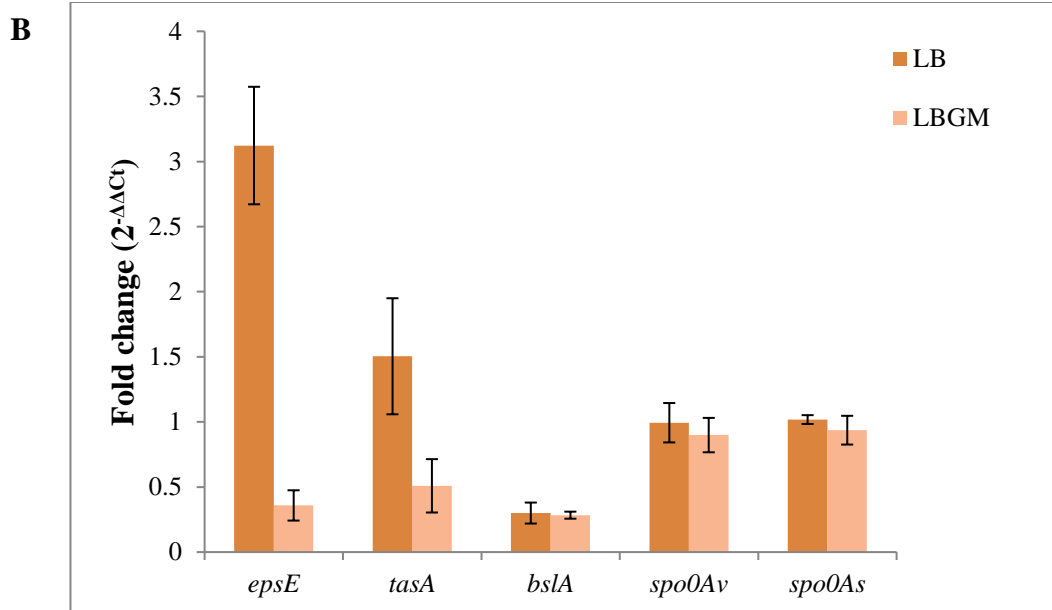


Fig. 3.13: Characterization of biofilm formation in *B. subtilis* DK1042 harbouring VHb (B) Relative quantification of mRNAs of *epsE*, *tasA*, *bslA*, *Spo0Av*, *Spo0As* in NRM1113 as compared to *B. subtilis* DK1042 WT (n=3, p≤0.05, error bars represent standard error of mean).

Flagella independent surface spreading on 1.5 % agar occurs due to osmotic pressure gradients generated by EPS secretion and outward pressure of cell growth facilitated by surfactin (Kearns, 2010; Seminara et al., 2012; Mhatre et al., 2017). We wished to elucidate the role of matrix producing genes in surface spreading in the integrant. Relative gene expression analysis (**Fig. 3.13, B**) in comparison to WT showed 64.17% (±11.6) downregulation of *epsE* gene in LBGM grown biofilm of NRM1113 while it was upregulated 3.12 (±0.45) fold in LB grown biofilm of NRM1113 (n = 3, p≤0.05). Differential regulation of *epsE* in NRM1113 depending upon different media conditions justifies the extent of colony expansion on LB and LBGM medium. Colony expansion on LB could be due to upregulation of *eps* operon as well as surfactin production while on LBGM it could chiefly be attributed to surfactin mediated sliding motility. *bslA* gene was downregulated 70.02% (±8.0) and 71.65% (±2.7) in LB and LBGM grown biofilm of NRM1113, respectively (n = 3, p≤0.05) (**Fig 3.13, B**).

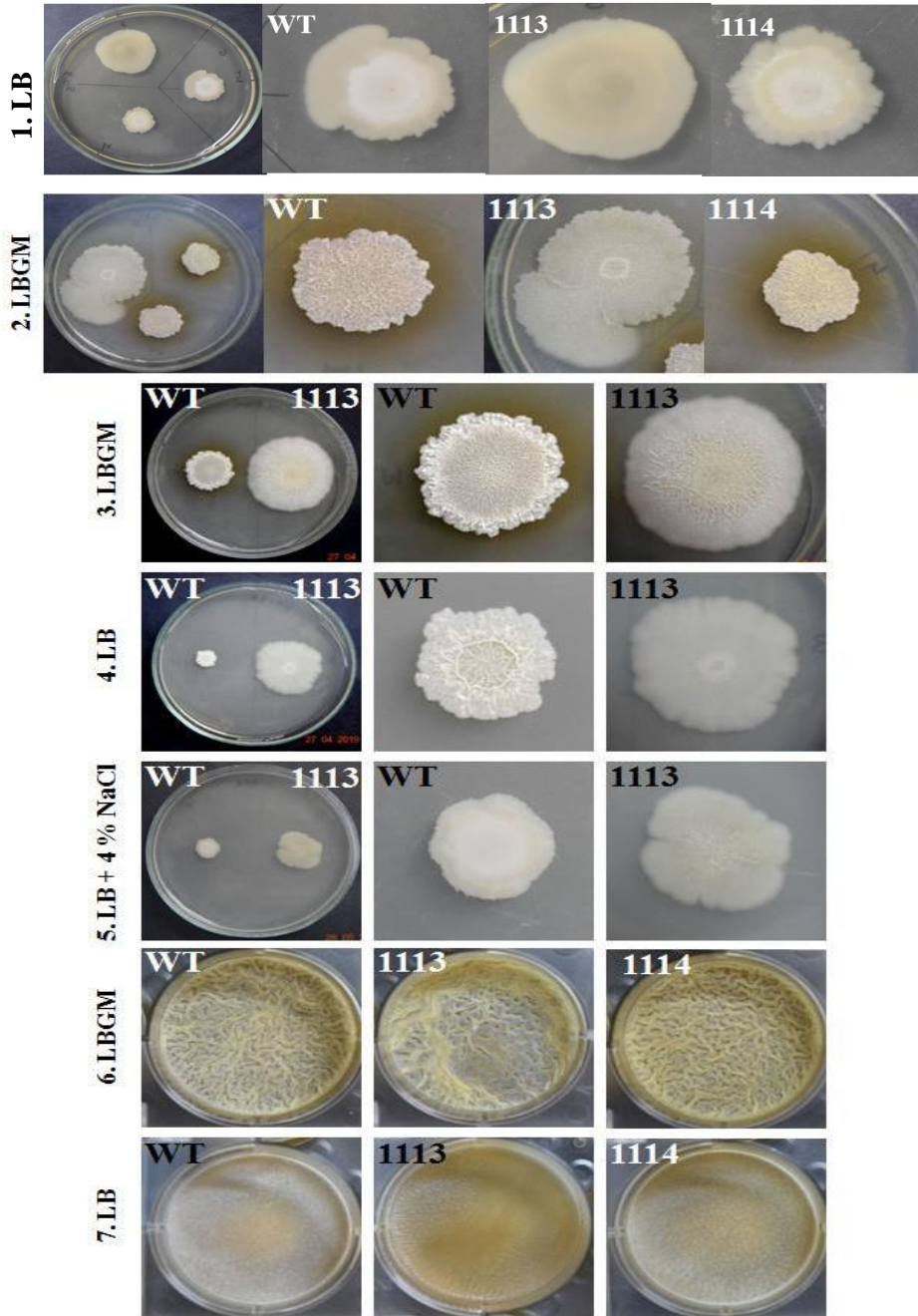


Fig. 3.14: Effect of *Vitreoscilla* haemoglobin on pellicle and colony biofilm formation by *B. subtilis* DK1042. Colony Morphology – (Panel 1 to 5). 1. LB agar 72h, 2. LBGM agar 72 h, 3. LBGM agar 72 h, 4. LB agar 72 h, 5. LB with 6% NaCl agar 72 h, Pellicle morphology – (Panel 6 and 7) 6. LBGM broth 48 h, 7. LB both 48 h.

This significant down-regulation of *bslA* in NRM1113 further strengthens the possibility of increased surfactin production because intermediate level of DegU~P activates *bslA* expression and lower level of DegU~P derepresses *urfA* operon leading to increased surfactin production which in turn facilitates surface spreading (Miras and Dubnau, 2016). Expression of *tasA* in NRM1113 was statistically insignificant with respect to WT in both the media conditions. Expression of *spo0A* transcripts from vegetative (*spo0Av*) as well as sporulation (*spo0As*) promoters was also similar in NRM1113 on LB and LBGM indicating that Vhb does not alter the transcription of *spo0A* and alterations in biofilm phenotype of integrant could mainly be due to change in the levels of Spo0A~P.

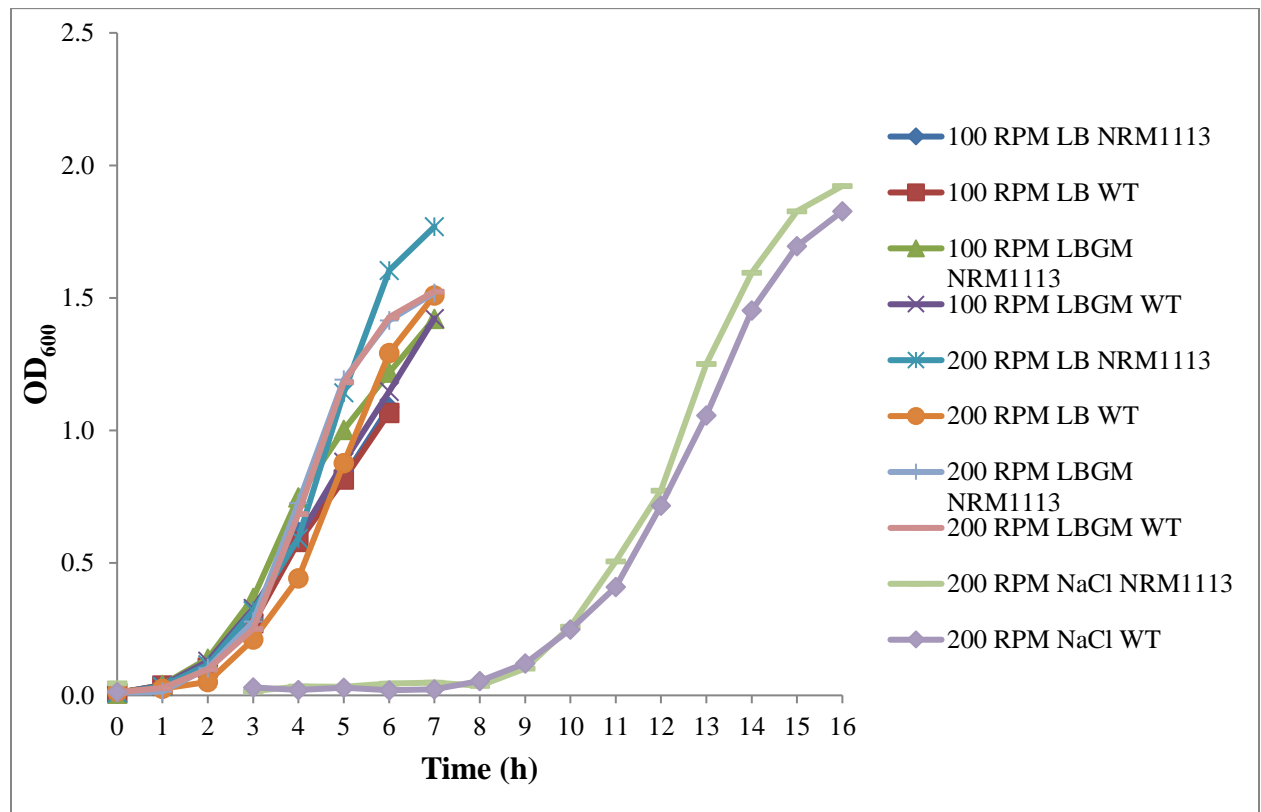


Fig. 3.15: Growth curves of *B. subtilis* DK1042 WT and NRM1113 in LB, LBGM and LB broth containing 6% NaCl at different shaking conditions at 30 °C.

Table 3.2: Growth curve characteristics of *B. subtilis* DK1042 and NRM1113 under medium and shaking different conditions.

Sr. No.	Growth Medium	Shaking condition (rpm)	Specific growth rate (h^{-1})		Doubling time (min)	
			WT	NRM1113	WT	NRM1113
1	LB	100	0.922	0.939	45.09	44.28
2	LBGm	100	1.037	1.151	40.09	36.12
3	LB	200	0.877	0.966	47.41	43.04
4	LBGm	200	1.045	1.157	39.78	35.93
5	LB with 6% NaCl	200	0.591	0.699	70.35	59.48

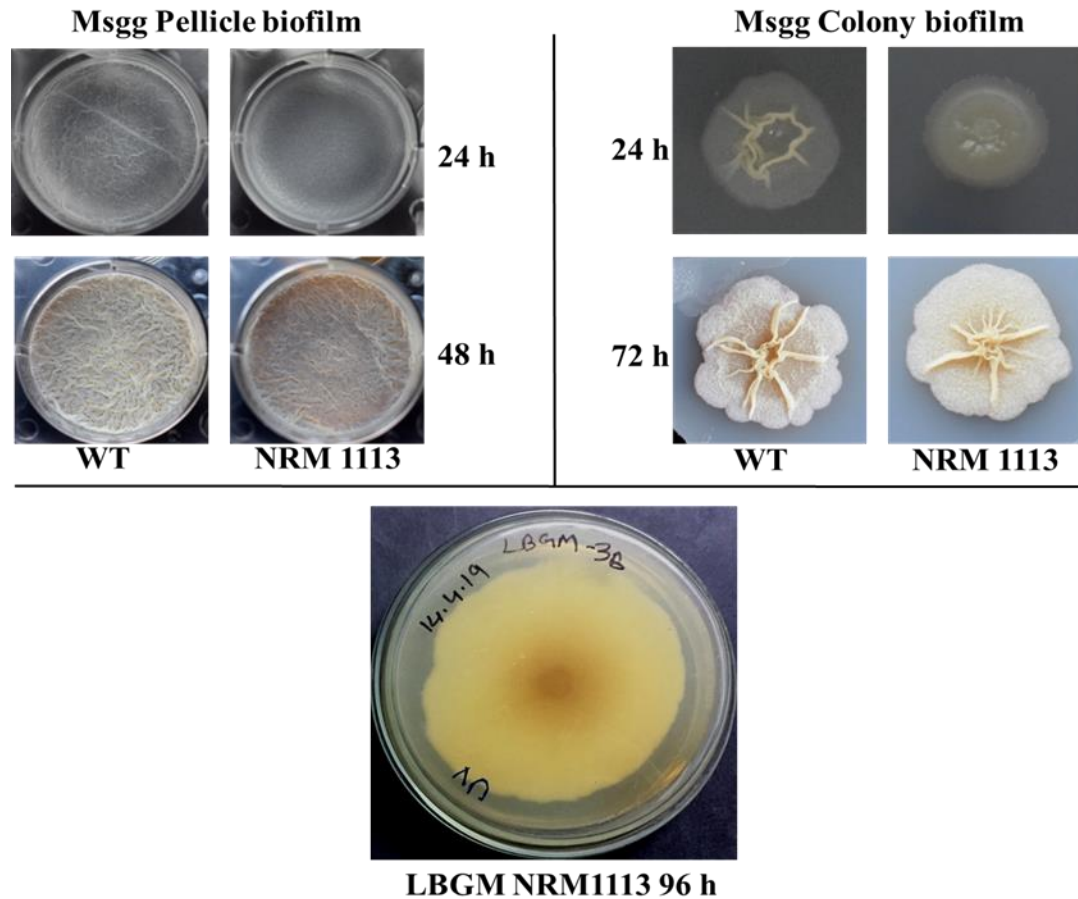


Fig. 3.16: Effect of Vhb on biofilm formation by *B. subtilis* DK1042 in Msgg medium.

3.4.4.2 Sporulation and production of brown pigment in DK1042 harboring VHb

Biofilm associated sporulation was less in NRM1113 than in WT on LB and LBGM agar (Fig. 3.17). The sporulation percentage for WT and NRM1113 was 0.91% and 0%, respectively, on LB at 72 h. On the other hand, the efficiency of sporulation was 87.2% in WT and 17.14% in NRM1113 on LBGM at 72 h. Precise mechanisms responsible for VHb driven alterations in biofilm formation and sporulation in NRM1113 remains to be determined but significant down-regulation of *bsIA* is responsible for the decrease in the complexity of colony biofilms and lack of biofilm maturity in turn reduced biofilm-associated sporulation in NRM1113 possibly via a checkpoint protein, KinD until mature biofilm is formed (Aguilar et al., 2010; Ostrowski et al., 2011).

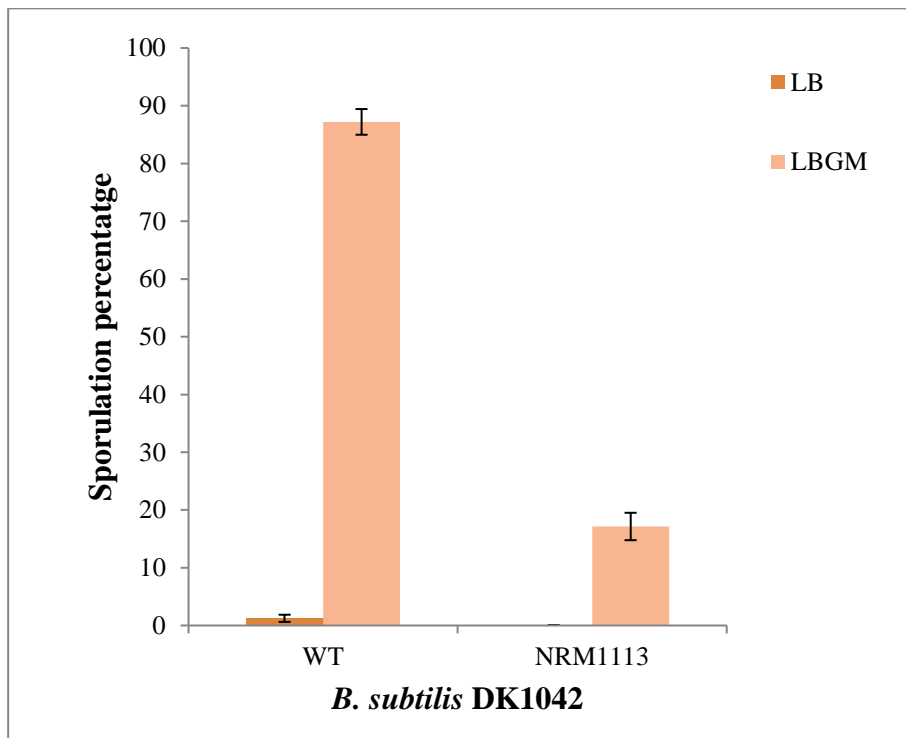


Fig. 3.17: Sporulation efficiencies of *B. subtilis* DK1042 WT and NRM1113 on LB and LBGM agar (1.5%) medium at 72 h. (n=1, $p \leq 0.05$, error bars represent standard deviation of mean).

Secretion of pulcherriminic acid was restricted to the leading edge of the NRM1113 biofilm but there was a distinct halo of pulcherriminic acid beyond the edge of the WT biofilm (**Fig. 3.18**). These results are well in accordance with the recent study linking the diffusion of pulcherriminic acid and pulcherrimin formation with the growth arrest of the biofilm in *B. subtilis* (Arnaouteli et al., 2019). The integrant started accumulating pulcherriminic acid in growth-limiting quantities similar to WT only after 96 h and that was limited to the center of the colony (**Fig. 3.16**). This raises the possibility of yet another unidentified stress signal that triggers the secretion and accumulation of pulcherriminic acid at growth limiting quantities in the integrant as the centre of the colony faces depletion of nutrients and oxygen and accumulation of toxic products (Stewart and Franklin, 2008). WT and NRM1113 produced similar pellicle morphology in LB and LBGGM broth (**Fig. 3.14, Panels 6 and 7**). However, pulcherriminic acid secretion was less in NRM1113 with reference to WT in LBGGM broth (**Fig. 3.18**).

Sporulation defective mutants do not produce brown pigment in *B. subtilis* (Piggot and Coote, 1976). Reduced brown pigmentation in M9 minimal medium (Kleijn et al., 2010) shake flask cultures corroborates that sporulation might be delayed/reduced in the integrant as compared to WT. VHb increased the levels of antioxidants such as ascorbate in *Arabidopsis* plants (Wang et al., 2009) and it also possesses peroxidase activity (Kvist et al., 2007). Antioxidant enzymes such as catalase and peroxidase contribute to tackle ROS mediated stress (Liao 2015; Khan et al., 2016). Increasing accessibility of oxygen to the respiratory chain by VHb stimulates electron transport thereby increasing NAD⁺/NADH ratio and ATP production in the host cell (Zhang et al., 2007; Stark et al., 2015). Upregulation of energy generating and biosynthetic pathways is associated with the early stages of biofilm formation (Pisithkul et al., 2019). Whether the observed effects in the integrant NRM1113 are due to improved energy and antioxidants status by VHb needs further investigation. The future challenges include elucidation of downstream signaling process with the multi-omics approach involving metabolomic, transcriptomic, and proteomic analyses.

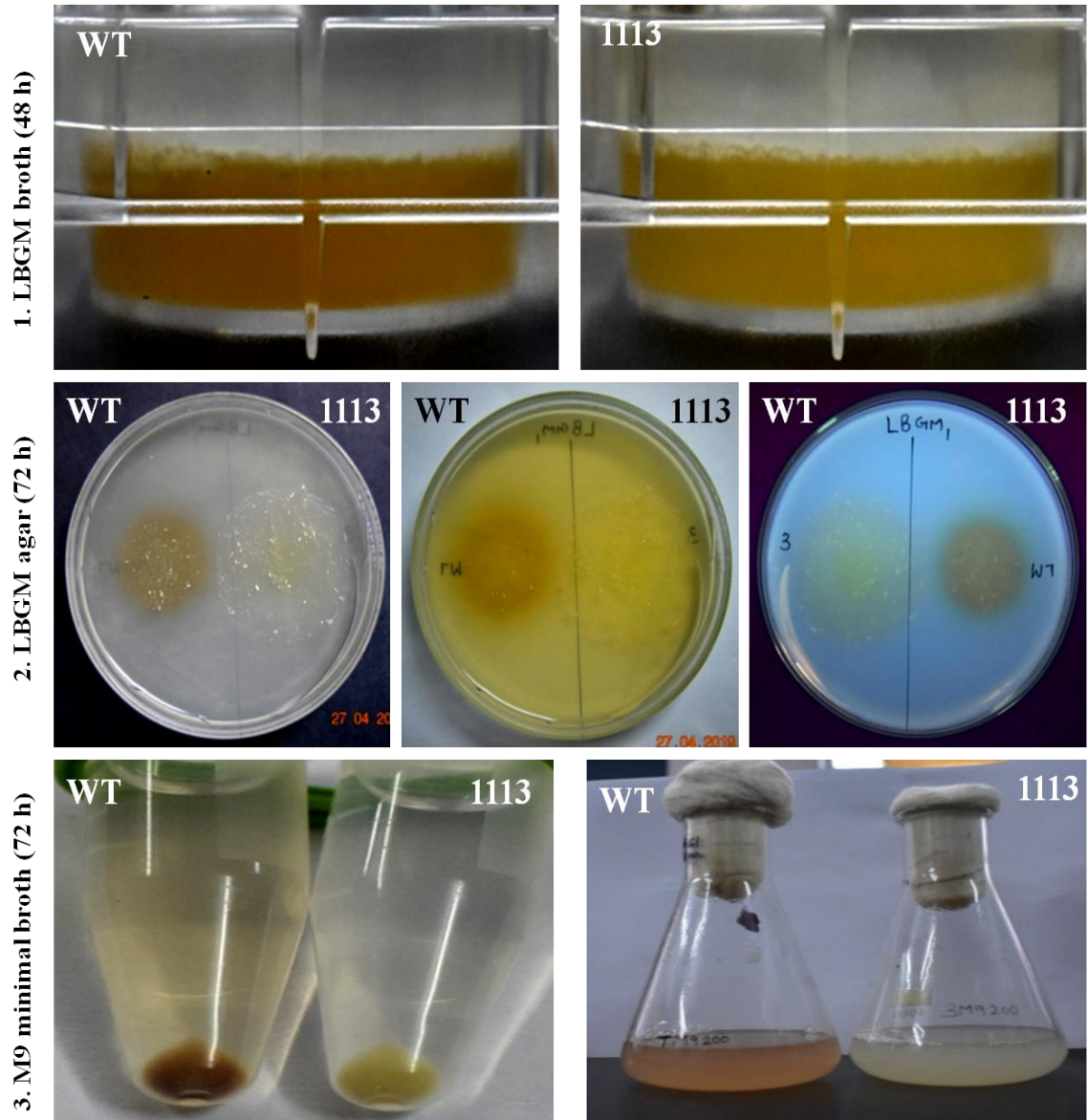


Fig. 3.18: Production of brown pigment by VHb harbouring *B. subtilis* DK1042.

3.5 Conclusion

Constitutive expression of VHb has resulted in the enhanced expansion of biofilm and reduced sporulation in *B. subtilis* DK1042. Sporulation is advantageous for *Bacillus* to survive under harsh conditions prevailing in soils but spore dormancy may shut off many genes and metabolic functions which are otherwise advantageous for promoting plant growth. Sporulation is the last resort for survival. Normal

physiological regime works in the direction of avoiding/delaying the sporulation (Schultz et al., 2009; Lo´pez et al., 2009; Gonza´lez-Pastor 2011). Use of multipromoter P43 repeats led to increase in the expression of GFP which can be inferred by comparing time and growth dependent analysis of GFP fluorescence in NRM1113 and NRM1114. However, NRM1113 outperformed NRM1114 in context of increase in biofilm formation and mitigation of sporulation. This could be due to unavailability of equal proportion of heme prosthetic group which is required for activity of apo Vhb. This means use of multipromoter system can enhance the expression of target genes cloned downstream of the promoter tandem repeats but it may not result in increased production of the final desired products or metabolites. In addition to this, biofilm formation is positively correlated with the biocontrol property and colonization ability of various strains of *Bacillus subtilis* on plant surfaces (Chen et al., 2012; Molina-Santiago et al., 2019). It would be interesting to see how do altered biofilm formation and sporulation influence root colonization and biocontrol property of Vhb containing *B. subtilis* DK1042.